Talanta 107 (2013) 140–145

Contents lists available at SciVerse ScienceDirect

Talanta

journal homepage: www.elsevier.com/locate/talanta

Label-free sensing of thrombin based on quantum dots and thrombin binding aptamer

Xiangyuan Zhang, Ruoxin Hu, Na Shao*

College of Chemistry, Beijing Normal University, Beijing 100875, PR China

ARTICLE INFO

Article history:
Received 16 September 2012
Received in revised form
2 January 2013
Accepted 4 January 2013
Available online 11 January 2013

Keywords:
CdTe quantum dots
Fluorescence recovery
Thrombin binding aptamer
Label-free
Thrombin

ABSTRACT

A facile and sensitive label-free approach for detection of thrombin based on CdTe quantum dots (QDs) and thrombin binding aptamer (TBA) is presented. The crude QDs can be "activated" with fluorescence enhancement by adding extra Cd^{2+} to the solution in basic medium. As a result, the positively charged Cd^{2+}-activating CdTe QDs could interact with the negatively charged TBA, leading to fluorescence quenching. When thrombin was added, TBA was induced to form a G-quadruplex structure and combined specifically with its target, releasing the QDs with a recovery of the fluorescence intensity. The sensing approach is based on the strongly specific interactions between TBA and thrombin over the electrostatic interactions between TBA and positively charged QDs. Based on the fluorescence enhancement of QDs, selective detection of thrombin was successfully achieved. A linear response for thrombin was observed in the range from 1.4 nM to 21 nM with a detection limit of 0.70 nM.

1. Introduction

Quantum dots (QDs) are semiconductor nanoparticles or alloys between 1 nm and 10 nm in size. Since its first appearance in 1983 [1], semiconductor QDs have been received broad research interest. Especially from 1998, when Chan and Nie [2] along with Bruchez et al. [3] prepared water soluble CdSe/ZnS core/shell QDs and utilized them for cellular imaging, researches focusing on biological applications of QDs have been paid increasing attention. Compared with conventional organic fluorophores, QDs display favorable photophysical properties, including size-controlled fluorescence, broad absorption and excitation spectra, narrow and symmetric fluorescence emission band, and high stability against photobleaching [4]. Thus, QDs have been widely utilized as excellent optical labels for biological imaging, sensing, and diagnostics [5–8].

The nature of the quantum dots surface is critical for photoluminescence properties. The fluorescence efficiency of the prepared QDs could be significantly reduced by localized surface trap states, especially for QDs synthesized in aqueous media [9]. In order to reduce non-radiative recombination, and to increase the photoluminescence efficiency, several methods could be used. For example, (1) Overcoating the QDs core with one or two semiconductor quantum shells with a larger band-gap [10]. (2) Surface passivation through treatments with metal ions like Cd^{2+} or Zn^{2+} [9]. (3) Photoactivation through exposure of QDs to UV or visible light [11].

Thrombin is a specific serine protease that plays a critical role in hemostasis. It converts soluble fibrinogen into insoluble strands of fibrin, as well as catalyzes many other coagulation-related reactions. Thrombin also has great importance in molecular biology, for instance, the recognition of tumor growth, metastasis, and angiogenesis [12]. Due to its biological significances, a lot of efforts have been done to develop simple and sensitive approach for detection of thrombin [13–19]. Among these, aptamer based methods are the mostly used strategies because of the excellent specificity of thrombin binding aptamer toward thrombin [20,21]. The 15-mer thrombin binding aptamer, with the sequence of 5′-GGTTGGTGTGGTTGG-3′, was selected from a randomized oligonucleotide library as a high affinity ligand for thrombin [22]. It could form a G-quadruplex structure consisting of two guanine quartets upon interactions with thrombin [23].

Different methodologies have been used to transduce the aptamer-target binding events to detectable physical signals, including colorimetry [24], electrochemistry [25,26], fluorescence spectra [27–29], capillary electrophoresis [30,31] and so on. However, in most methods, the aptamers were usually either modified with fluorophores or fixed onto a certain surface, like electrodes, through covalent coupling reactions, using the specific interactions between streptavidin and biotin, NHS and EDC, SH and metal elements like Au or Cd^{2+}, etc. Such covalent modifications are usually labor-intensive and time-consuming, and also it would lower the binding abilities of aptamers toward targets

* Corresponding author. Tel.: +86 10 58802146.
E-mail address: shaona@bnu.edu.cn (N. Shao).

0039-9140/$ - see front matter © 2013 Elsevier B.V. All rights reserved.
http://dx.doi.org/10.1016/j.talanta.2013.01.003

[32,33]. A large number of the methods reported were based on turn-off signals, which would lower the sensitivity of the probes due to the relatively high background with the decrease of intensity [34]. Here, we designed a label-free turn-on type fluorescent method to detect thrombin via monitoring the fluorescence changes of QDs induced by thrombin upon binding with its aptamer. This method for thrombin sensing has advantages of easy operation due to the elimination of complicated covalent modifications. The absence of modification could ensure the free conformational change of the aptamer when interacting with thrombin, thus leading to high binding affinity and sensitive detection. The results showed that this method was highly sensitive and selective in thrombin sensing, even in a complex biological matrix like serum.

2. Experimental section

2.1. Materials and reagents

Tellurium powder (approximately 325 mesh, 99.99%), 3-mercaptopropionic acid (3-MPA, 99%), and quinine hemisulfate monohydrate (99%) were from Alfa-Aesar. Cadmium chloride hemipentahydrate ($CdCl_2 \cdot 2.5\ H_2O$) and sodium borohydride (96%) were purchased from Sinopharm Chemical Reagent Company. Thrombin was purchased from Sigma. 15-mer thrombin binding aptamer (TBA) with the sequence of 5′-GGTTGGTGTGGTTGG-3′ was synthesized by Beijing Dingguo Biotechnology Company and was stored in 10 mM Tris–HCl buffer (pH=7.4) containing 1 mM ethylenediaminetetraacetic acid. Bovine serum albumin (BSA), lysozyme and immunoglobin G (IgG) were also purchased from Beijing Dingguo Biotechnology Company. Tris (hydroxymethyl) aminomethane (Tris) was purchased from Novon, Incorporation. Sulfuric acid, hydrochloric acid, sodium hydroxide, ethanol, and 2-propanol of analytical grade were all from Beijing Beihua Fine Chemical Company. The fresh human blood samples from healthy subjects were supplied by the affiliated hospital of Beijing Normal University. After careful settlement for 2 h, the supernatant was extracted as serum and then centrifuged thrice (2500 rpm, 10 min once). The serum samples were diluted five times prior to detection. The ultrapure water used throughout the experiments has a resistivity of more than 18 MΩ cm.

2.2. Apparatus

Fluorescence spectra were recorded using a Hitachi F-4600 fluorescence spectrometer, and UV–visible absorption spectra were recorded on a TU-1901 diode-array spectrophotometer. High-resolution transmission electron microscopy (HRTEM) was performed on a JEM-2010 (JEOL, Japan) electron microscope operating at 200 kV. The pH values of solution were determined by a REX PHS-3C pH meter. A stirrer with temperature sensor and a thermometer was used to control the temperature precisely.

2.3. Preparation of CdTe QDs

The CdTe QDs were prepared via a green synthetic route according to the reported method [35] with minor modification. Briefly, under a N_2 atmosphere, absolute ethanol (3 mL) was added to tellurium (6.8 mg) and excess sodium borohydride (18 mg) under magnetic stirring, which is kept at 70 °C for 1.5 h. The resulting pink ethanol solution of NaHTe was reacted with H_2SO_4 (50 mM, 5 mL) to produce H_2Te gas. Under stirring, H_2Te gas was introduced into the oxygen-free $CdCl_2$ (3.03 mM, 50 mL) aqueous solution containing 3-mercaptopropionic acid (MPA) (45 μL) stabilizer at pH 9.0 by a N_2 flow, resulting in the CdTe precursor solution. The initial molar ratio of Cd/Te/MPA was approximately 3:1:10. Then the above obtained CdTe precursor solution was refluxed at 100 °C for 5 h under open air conditions with a condenser attached. Calculated by the first absorption maximum according to a reported method [36], the CdTe QDs obtained were 3.0 nm in size. Isolation of 3-MPA capped CdTe QDs from their crude solution was achieved by precipitation with an equal volume of 2-propanol, and the sediment was collected by centrifugation at 6000 rpm for 5 min. This procedure was repeated for three times before the sediment was redissolved in double distilled water and then stored at 4 °C for the subsequent experiments.

Then the as-prepared CdTe QDs were characterized by high resolution transmission electron microscopy (HRTEM), absorption and fluorescence spectroscopies, respectively. The photoluminescence quantum yield (QY) of CdTe QDs was estimated using quinine sulfate (QY=54.6%) [37] as reference.

2.4. Thrombin detection

The originally prepared QDs were first activated as following: The solution of the QDs was adjusted to pH 10.5 by addition of 0.5 M NaOH; then, certain amount of extra $Cd(ClO_4)_2$ solution was added. The reaction was monitored by determining the fluorescence intensity excited at 370 nm. The addition of Cd^{2+} stopped when the fluorescence intensity no longer showed obvious increase.

After QDs activation was performed under optimum conditions, TBA (4.35 μM, final concentration) was added into the Cd^{2+}-activating CdTe QDs solution. And then, the emission spectra were recorded after 30 min of equilibration time. Then, for thrombin detection, different concentrations of thrombin were added into the above Cd^{2+}-activating CdTe QDs–aptamer solution with incubation at 37 °C for 30 min, and then the fluorescence intensity was monitored.

Each measurement was conducted three times to estimate the error value of one data point.

3. Results and discussion

3.1. Characterization of CdTe QDs

The photo-physical properties of the as-prepared QDs were characterized using UV–visible absorption spectra and fluorescence emission spectra, as illustrated in Fig. 1. The absorption maximum of the first electronic transition was at 520 nm. The fluorescence spectra of the CdTe QDs showed an emission maximum at 563 nm upon excitation at 370 nm. The well-resolved sharp first excitonic peak in the absorption spectra and narrow FWHM (full width at half maximum) in the fluorescence emission spectra indicated a narrow size distribution of the as-prepared CdTe QDs [38]. The photoluminescence quantum yield (QY) of the CdTe QDs was determined to be 19%.

High resolution transmission electron micrograph (HRTEM) was employed to characterize the morphology of the as-synthesized CdTe QDs, as was shown in Fig. 2. The CdTe nanocrystals appeared as roughly spherical particles and possessed a relatively good monodispersity and crystallinity. The average diameter of the CdTe nanoparticles was 3.2 nm ± 0.2 nm.

3.2. Efficient activation effect of Cd^{2+} on CdTe QDs

The activation of QDs is typically attributed to some forms of surface passivation. In this paper, surface passivation via treatment of QDs with metal ions was applied due to its high efficiency and convenience. Upon addition of Cd^{2+}, surface defect states were passivated, and the CdTe QDs were thus activated

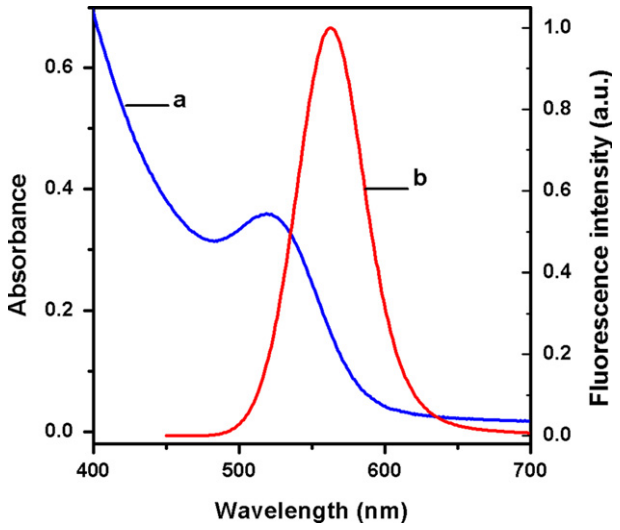

Fig. 1. UV–visible absorption (a) and fluorescence emission (b) spectra of the prepared MPA-capped CdTe QDs. The excitation wavelength was 370 nm.

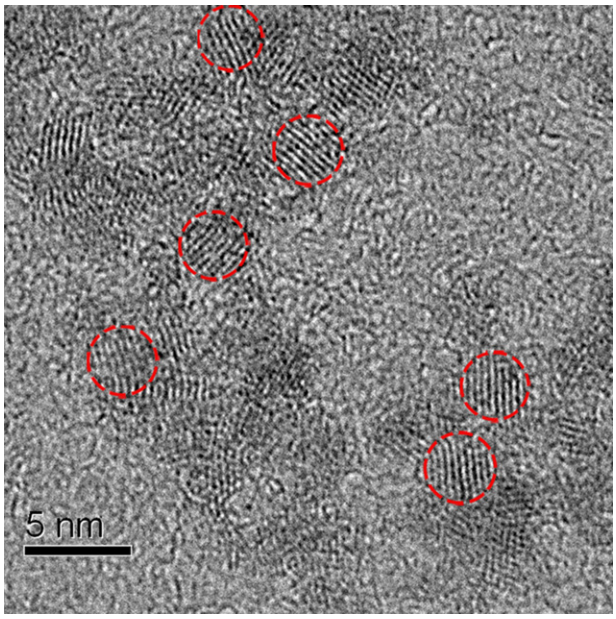

Fig. 2. HRTEM image of the as-prepared CdTe QDs with MPA as stabilizers.

[39,40]. Consequently, the fluorescence intensity was enhanced. The factors influencing the activation effect were studied as following.

In our experiment, the fluorescence enhancement of CdTe QDs by Cd^{2+} could be achieved only in a relatively narrow pH ranging from 9 to 12, and the optimal activation effect was obtained at pH 10.5. Under relatively low pH conditions, the protonation of the ligand 3-mercaptopropionic acid will cause the dissociation of surface ligands and subsequently the aggregation of CdTe QDs [41]. When the pH was higher than 12, the added Cd^{2+} tended to bind with OH^- to form $Cd(OH)_2$, rather than adsorb on the QDs surface.

The amount of Cd^{2+} added played a critical role in the activation effect. Throughout the course of titrations, the maximum emission wavelength centered at about 570 nm with shift less than $\pm$5 nm. The fluorescence intensity increased gradually with Cd^{2+} concentration increasing at first, and then leveled off at higher concentration of Cd^{2+}, as presented in Fig. 3(a). The maximum enhancement occurred at Cd^{2+} to QDs ratio of ca. 13 (50 μM Cd^{2+} added into 4.0 μM QDs solution). According to the fitting method reported [42], the effects of the added Cd^{2+} on the CdTe QDs fluorescence enhancement could be well described by a typical Langmuir adsorption model, as shown in Fig. 3(b), which indicated that there were only a finite number of vacant binding sites on the surface of the QDs.

The activation time was also studied. The fluorescence intensity of the 4.0 μM CdTe QDs solution with 54.3 μM Cd^{2+} added reached maximum 20 min later.

3.3. Interactions between TBA and Cd^{2+}-activating CdTe QDs

The fluorescence intensity of the Cd^{2+}-activating CdTe QDs solution was obviously quenched upon addition of TBA. This was considered to be the result of adduct formation between TBA and QDs that resulted in the loosely-bound Cd^{2+} being displaced from the nanoparticle surface by the counterion TBA brought (Na^+) [43]. Although fluorescence quenching was also observed in the original CdTe QDs solution without Cd^{2+} activation, the fluorescence intensity changes of Cd^{2+}-activating CdTe QDs upon addition of TBA was evidently greater than that of the original CdTe QDs, as depicted in Fig. 4. This further proved that the interactions between CdTe QDs and TBA was dominated by the electrostatic forces between the cationic Cd^{2+}-activating QDs surface and the negatively charged TBA backbone [44,45]. This result is consistent with that reported by Murphy's group [46].

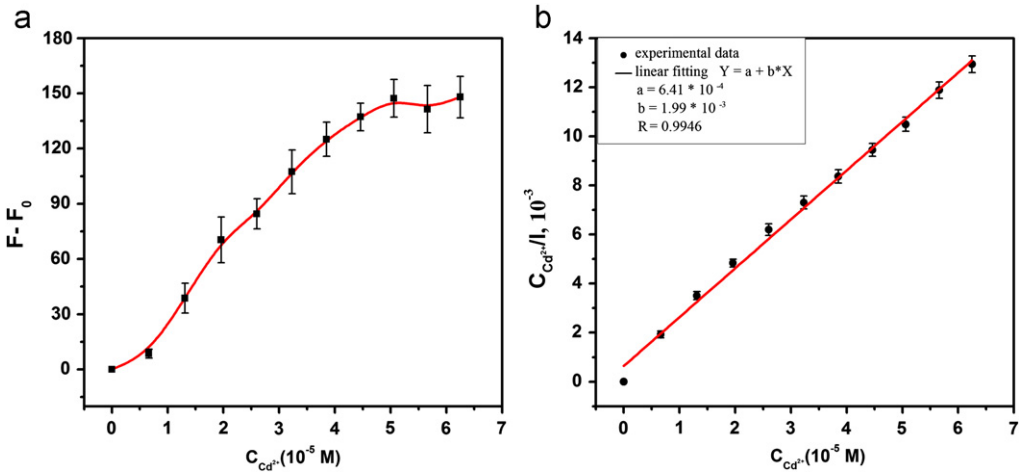

Fig. 3. (a) Fluorescence intensity changes of the activated CdTe QDs as a function of the concentration of Cd^{2+}, (b) Langmuir adsorption plots for the CdTe QDs with different concentrations of added Cd^{2+} solutions. (F_0 and F are the fluorescence intensity of CdTe QDs before and after Cd^{2+} activation, respectively.)

3.4. Label-free assay of thrombin

3.4.1. Detection mechanism

The sensing mechanism of the present approach for thrombin detection is described in Scheme 1. The fluorescence emission of the CdTe QDs could be enhanced significantly by adding some amount of Cd^{2+} under basic conditions (as was shown in Fig. 5, Line a and b), due to the effective passivation of surface defects on the CdTe QDs. And the fluorescence of the Cd^{2+}-activating QDs could be quenched (Fig. 5, Line c) when it interacted with the negatively charged TBA through electrostatic interactions. When thrombin was added, the TBA was induced to form G-quadruplexes to bind with thrombin owing to the specific binding interactions [20,21], and the CdTe QDs were released with an increase of fluorescence intensity (Fig. 5, Line d). Based on the fluorescent signal changes of CdTe QDs when TBA specifically interacted with thrombin, label-free sensing of thrombin was thus achieved.

3.4.2. Detection of thrombin

For sensing of thrombin, different concentration of thrombin was added into the solution containing Cd^{2+}-activating CdTe QDs and TBA. The fluorescence intensity initially increased rapidly with adding thrombin at lower concentration, and then followed by a slow rise at higher concentration of thrombin over 20 nM (Fig. 6).

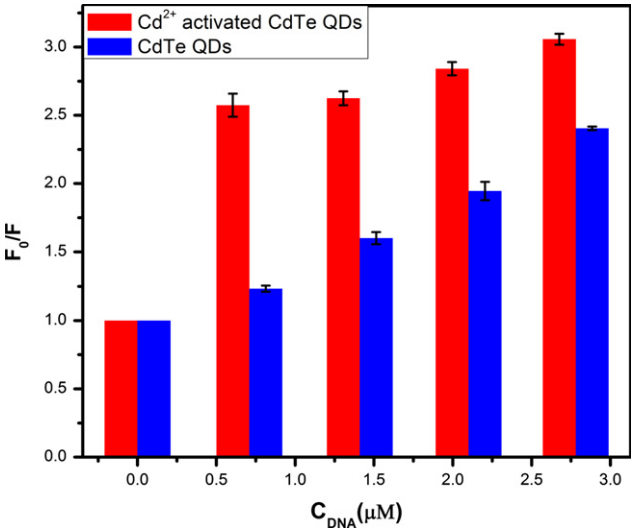

Fig. 4. Comparison of the quenching effects of TBA on the fluorescence of the original CdTe QDs and the Cd^{2+}-activating CdTe QDs. (F_0 and F are the fluorescence intensity before and after TBA was added, respectively.)

It was found that the fluorescence intensity enhancement displayed a linear relationship with the thrombin concentration in the range from 1.4 nM to 21 nM (R=0.9952, inset of Fig. 6), suggesting that this approach could be used for label-free quantification of thrombin. The detection limit of thrombin was determined to be 0.70 nM based on a linear fitting and the noise level of 3σ where σ is the standard deviation of Cd^{2+}–CdTe–aptamer fluorescence measured at 0 nM thrombin.

3.4.3. Interference study

The fluorescence changes of the Cd^{2+}–CdTe–aptamer system towards three other proteins, including BSA, lysozyme and IgG, were also examined. As presented in Fig. 7, when thrombin was added, the fluorescence intensity was remarkably enhanced (bar b). While when BSA, lysozyme or IgG was added, nearly no changes of the fluorescence intensity were observed (Fig. 7, bar c–e). To further test the responsive specificity, the effects of several inorganic metal ions on this system were also examined. As shown in Table 1, the tolerable concentrations of the QDs–TBA system towards metal ions were all beyond the concentration ranges in healthy subjects. These results revealed that the approach developed here could show highly selective response toward thrombin, free from the interferences of common coexisting inorganic ions or proteins.

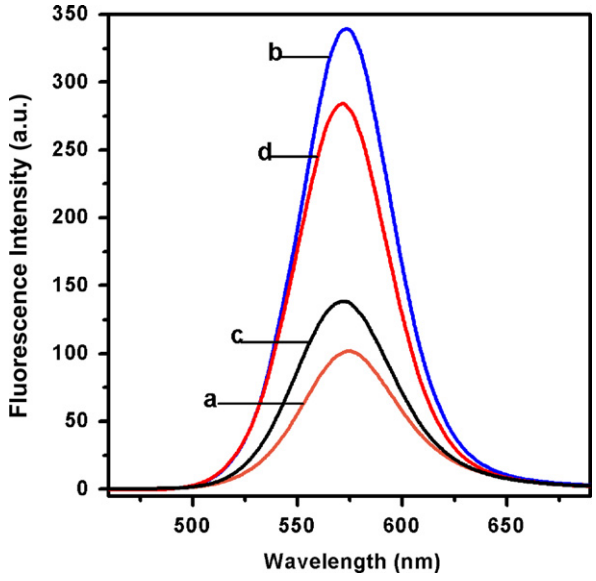

Fig. 5. Fluorescence emission spectra: (a) CdTe QDs, (b) CdTe QDs+Cd^{2+}, (c) CdTe QDs+Cd^{2+}+TBA, (d) CdTe QDs+Cd^{2+}+TBA+thrombin. [CdTe QDs]=4.0 μM, [Cd^{2+}]=54.3 μM, [TBA]=4.35 μM, [thrombin]=28.6 nM. The excitation wavelength was 370 nm.

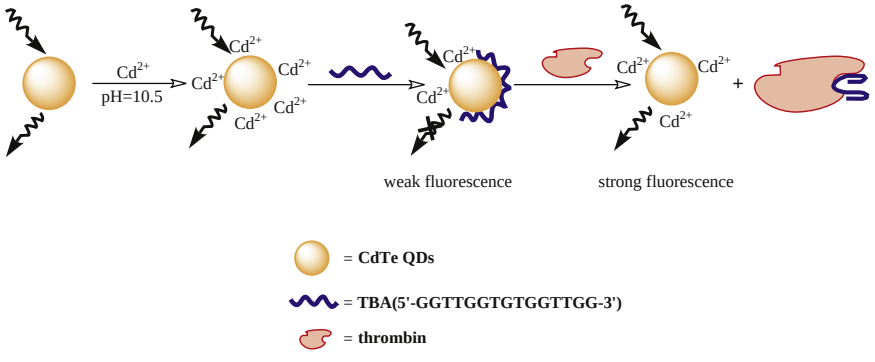

Scheme 1. Possible mechanism of the aptamer based sensor using CdTe QDs as fluorescent probe.

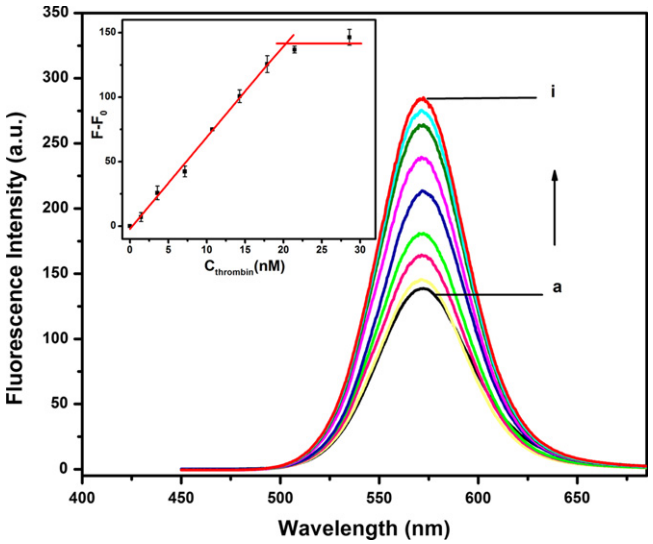

Fig. 6. Fluorescence emission spectra of Cd^{2+}-activating QDs containing TBA at thrombin concentrations of 0, 1.43, 3.58, 7.15, 10.73, 14.29, 17.87, 21.45, and 28.6 nM (a–i). Inset graph: relationship between the fluorescence intensity of CdTe–aptamer and different concentrations of thrombin. (F_0 and F are the fluorescence intensity of Cd^{2+}-activating QDs containing TBA in the absence and presence of thrombin, respectively.) [CdTe QDs]=4.0 μM, [Cd^{2+}]=54.3 μM, [TBA]=4.35 μM. The excitation wavelength was 370 nm.

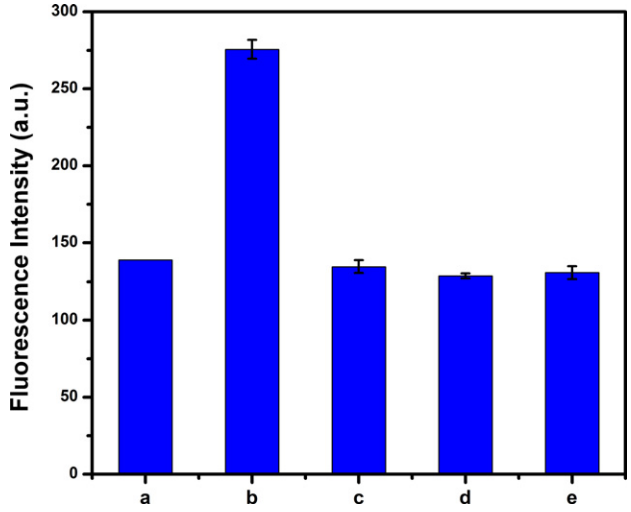

Fig. 7. Responsive selectivity of QDs–aptamer to different substances studied. (a) CdTe QDs+TBA, (b–e) CdTe QDs+TBA+different proteins: (b) thrombin, (c) BSA, (d) lysozyme, (e) IgG. [CdTe QDs]=4.0 μM, [Cd^{2+}]=54.3 μM, [TBA]=4.35 μM, [protein]=20 nM. The excitation wavelength was 370 nm.

Table 1
The interference of possible metal ions on the detection of thrombin.

Metal ions	Concentrations in healthy human serum	Tolerable concentration	$\Delta I/I$ (%) [a]
Na^+	136–145 mM	145 mM	−2.22
K^+	3.5–5.5 mM	5.5 mM	1.55
Ca^{2+}	2.25–2.75 mM	2.75 mM	−0.55
Mg^{2+}	0.7–1.1 mM	1.35 mM	0.287
Zn^{2+}	7.65–23 μM	56.69 μM	0.144
Fe^{2+}	10.7–30.4 μM	10 μM	−1.53
Fe^{3+}		31 μM	−2.72

[a] $\Delta I=I-I_0$, where I_0 and I are the fluorescence intensities of the QDs–aptamer system in the absence and presence of metal ions.

Table 2
Thrombin assay in human serum samples.

Sample	Spiked (nM)	Found (nM)	Recovery (%)	RSD (%)
Serum 1	1.55	1.62	104.5	8.40
Serum 2	8.86	9.14	103.2	5.52
Serum 3	15.5	14.73	95.03	2.65

Each sample was repeated for three times and averaged to obtain the recovery and RSD values. All human serum samples were diluted 5-fold prior to assay.

3.4.4. *Thrombin detection in human serum sample*

To demonstrate the capability of the proposed method in complex biological matrix, the detection of thrombin in 5-fold-diluted serum samples were conducted. As no coagulation proteins were contained in healthy human serum samples, no thrombin was detected in the serum. Therefore, we spiked the 5-fold-diluted serum samples with different concentrations of thrombin: 1.55 nM, 8.86 nM and 15.5 nM, respectively. The thrombin concentration in serum was derived from the working curve (Fig. 6, inset graph). And the recoveries were obtained by comparing the measured amounts to that of added thrombin, which varied from 95% to 104.5%, as was shown in Table 2. These results demonstrated that the QDs–aptamer system developed here could efficiently monitor thrombin concentration, even in complex serum samples.

4. Conclusions

In summary, we have developed a new QDs–aptamer sensing system for specific detection of thrombin. The addition of Cd^{2+} to the CdTe QDs solution may occupy the Cd^{2+} vacant sites on the QDs surface to offset the surface defects, resulting in enhanced fluorescence emission. The Cd^{2+}-activating QDs possessing a positively charged surface could bind with the negatively charged thrombin binding aptamer (TBA) via electrostatic forces, resulting in significant fluorescence quenching. When thrombin was added, TBA changed configuration to bind specifically with its target, releasing previously bound QDs, and a turn-on fluorescence signal was observed. Consequently, based on the fluorescence changes of QDs, a simple aptamer based label-free method for sensing of thrombin was achieved.

The QDs–aptamer fluorescent sensing approach developed here offers several advantages over works reported before. First, this method was easy to perform as complicated covalent modification was avoided. Second, the turn-on sensing mode could reduce background signal and improve sensitivity. Third, it is simple for thrombin detection in real serum samples, requiring no pretreatment or separation of the serum matrix. Last but not least, this approach developed here may offer a new and relatively general approach to proteins and small molecule analytes detection by changing into other aptamer systems.

Acknowledgements

This work was supported by the National Natural Science Foundation of China (No. 20905008), Research Fund for the Doctoral Program of Higher Education of China (No. 20090003120007).

References

[1] R. Rossetti, S. Nakahara, L.E. Brus, J. Chem. Phys. 79 (1983) 1086–1088.
[2] W.C.W. Chan, S.M. Nie, Science 281 (1998) 2016–2018.
[3] M. Bruchez, M. Moronne, P. Gin, S. Weiss, A.P. Alivisatos, Science 281 (1998) 2013–2016.

[4] X. Wu, H. Liu, J. Liu, K.N. Haley, J.A. Treadway, J.P. Larson, N. Ge, F. Peale, M.P. Bruchez, Nat. Biotechnol. 21 (2002) 41–46.
[5] W.T. Al-Jamal, K.T. Al-Jamal, B. Tian, L. Lacerda, P.H. Bomans, P.M. Frederik, K. Kostarelos, ACS Nano 2 (2008) 408–418.
[6] L.D. Chen, J. Liu, X.F. Yu, M. He, X.F. Pei, Z.Y. Tang, Q.Q. Wang, D.W. Pang, Y. Li, Biomaterials 29 (2008) 4170–4176.
[7] J. Wang, G. Liu, A. Merkoçi, J. Am. Chem. Soc. 125 (2003) 3214–3215.
[8] J.A. Hansen, R. Mukhopadhyay, J.Ø. Hansen, K.V. Gothelf, J. Am. Chem. Soc. 128 (2006) 3860–3861.
[9] L. Spanhel, M. Haase, H. Weller, A. Henglein, J. Am. Chem. Soc. 109 (1987) 5649–5655.
[10] A.R. Kortan, R. Hull, R.L. Opila, M.G. Bawendi, M.L. Steigerwald, P.J. Carroll, L.E. Brus, J. Am. Chem. Soc. 112 (1990) 1327–1332.
[11] S. Dembski, C. Graf, T. Krüger, U. Gbureck, A. Ewald, A. Bock, E. Rühl, Small 4 (2008) 1516–1526.
[12] M.L. Nierodzik, S. Karpatkin, Cancer Cell 10 (2006) 355–362.
[13] D.W. Huang, C.G. Niu, P.Z. Qin, M. Ruan, G.M. Zeng, Talanta 83 (2010) 185–189.
[14] V. Pavlov, Y. Xiao, B. Shlyahovsky, I. Willner, J. Am. Chem. Soc. 126 (2004) 11768–11769.
[15] R. Polsky, R. Gill, L. Kaganovsky, I. Willner, Anal. Chem. 78 (2006) 2268–2271.
[16] R. Nutiu, Y. Li, J. Am. Chem. Soc. 125 (2003) 4771–4778.
[17] L.W. Dick Jr, L.B. McGown, Anal. Chem. 76 (2004) 3037–3041.
[18] L.C. Chen, C.W. Chi, Y.H. Lao, Y.S. Li, Biosens. Bioelectron. 26 (2011) 3346–3352.
[19] J. Zheng, J.S. Li, Y. Jiang, J.Y. Jin, K.M. Wang, R.H. Yang, W.H. Tan, Anal. Chem. 83 (2011) 6586–6592.
[20] J.J. Li, X. Fang, W. Tan, Biochem. Biophys. Res. Commun. 292 (2002) 31–40.
[21] E.G. Guignet, R. Hovius, H. Vogel, Nat. Biotechnol. 22 (2004) 440–444.
[22] L.C. Bock, L.C. Griffin, J.A. Latham, E.H. Vermaas, J.J. Toole, Nature 355 (1992) 564–566.
[23] I. Smirnov, R.H. Shafer, Biochemistry 39 (2000) 1462–1468.
[24] H. Wei, B. Li, J. Li, E. Wang, S. Dong, Chem. Commun. (2007) 3735–3737.
[25] H. Yang, J. Ji, Y. Liu, J.L. Kong, B.H. Liu, Electrochem. Commun. 11 (2009) 38–40.
[26] Y. Xiao, A.A. Lubin, A.J. Heeger, K.W. Plaxco, Angew. Chem. Int. Ed. 44 (2005) 5456–5459.
[27] H. Chang, L. Tang, Y. Wang, J. Jiang, J. Li, Anal. Chem. 82 (2010) 2341–2346.
[28] H. Dong, W. Gao, F. Yan, H. Ji, H. Ju, Anal. Chem. 82 (2010) 5511–5517.
[29] J.H. Choi, K.H. Chen, M.S. Strano, J. Am. Chem. Soc. 128 (2006) 15584–15585.
[30] M.Y. Song, Y.X. Zhang, T. Li, Z.X. Wang, J.F. Yin, H.L. Wang, J. Chromatogr. A 1216 (2009) 873–878.
[31] H.Q. Zhang, X.F. Li, X.C. Le, J. Am. Chem. Soc. 130 (2008) 34.
[32] T. Li, R. Fu, H.G. Park, Chem. Commun. 46 (2010) 3271–3273.
[33] P. Song, Y. Xiang, H. Xing, Z. Zhou, A. Tong, Y. Lu, Anal. Chem. 84 (2012) 2916–2922.
[34] J.R. LAKOWICZ, (2008).
[35] N. Gaponik, D.V. Talapin, A.L. Rogach, K. Hoppe, E.V. Shevchenko, A. Kornowski, A. Eychmuller, H. Weller, J. Phys. Chem. B 106 (2002) 7177–7185.
[36] W.W. Yu, L. Qu, W. Guo, X. Peng, Chem. Mater. 15 (2003) 2854–2860.
[37] W. Melhuish, J. Phys. Chem. 65 (1961) 229–235.
[38] C.H. Fischer, H. Weller, A. Fojtik, C. LumePereira, E. Janata, A. Henglein, Ber. Bunsen. Ges. Phys. Chem 90 (1986) 46–49.
[39] D.E. Moore, K. Patel, Langmuir 17 (2001) 2541–2544.
[40] D.J. Zhou, Y. Li, E.A.H. Hall, C. Abell, D. Klenerman, Nanoscale 3 (2011) 201–211.
[41] J. Aldana, N. Lavelle, Y. Wang, X. Peng, J. Am. Chem. Soc. 127 (2005) 2496–2504.
[42] Y. Chen, Z. Rosenzweig, Anal. Chem. 74 (2002) 5132–5138.
[43] M.A. Berg, R.S. Coleman, C.J. Murphy, Phys. Chem. Chem. Phys. 10 (2008) 1229–1242.
[44] R. Mahtab, S.M. Sealey, S.E. Hunyadi, B. Kinard, T. Ray, C.J. Murphy, J. Inorg. Biochem. 101 (2007) 559–564.
[45] J.R. Lakowicz, I. Gryczynski, Z. Gryczynski, K. Nowaczyk, C.J. Murphy, Anal. Biochem. 280 (2000) 128–136.
[46] R. Mahtab, H.H. Harden, C.J. Murphy, J. Am. Chem. Soc. 122 (2000) 14–17.